Random matrix study of the phase structure of QCD with two colors

Benoît Vanderheyden[1,2] and A. D. Jackson[1]
[1] *The Niels Bohr Institute, Blegdamsvej 17, DK-2100 Copenhagen Ø, Denmark.*
[2] *Institut d'Electricité Montefiore, Campus du Sart-Tilman B-28, B-4000 Liège, Belgium.*
(August 12, 2009)

We apply a random matrix model to the study of the phase diagram of QCD with two colors, two flavors, and a small quark mass. Although the effects of temperature are only included schematically, this model reproduces most of the ground state predictions of chiral perturbation theory and also gives a qualitative picture of the phase diagram at all temperatures. It leads, however, to an unphysical behavior of the chiral order parameter and the baryon density in vacuum and does not support diquark condensation at arbitrarily high densities. A better treatment of temperature dependence leads to correct vacuum and small temperature properties. We compare our results at both high and low densities with the results of microscopic calculations using the Nambu-Jona-Lasinio model and discuss the effects of large momentum scales on the variations of condensation fields with chemical potential.

I. INTRODUCTION

A number of early and recent model calculations [1–4] indicate that quark-quark correlations may play an important role in QCD at finite density. By inducing pairing gaps $\Delta \sim 100$ MeV, such correlations may prove relevant for the physics of neutron and compact stars as well as that of heavy-ion collisions [2–8]. Due to the limitations of standard Monte Carlo techniques when applied to systems with finite baryon density, the study of these effects through lattice simulations is very challenging. A non-zero chemical potential leads to a complex determinant of the Euclidean Dirac operator and results in massive cancellations among configurations. This difficult problem stands in the way of a qualitative understanding of the critical physics involved in lattice simulations [9].

One response to this situation is to consider QCD-like theories with additional antiunitary symmetries that guarantee the reality of the fermion determinant and therefore render such theories more amenable to lattice formulations. Examples of such theories include QCD with an arbitrary number of colors, N_c, and adjoint quarks as well as QCD with two colors and fundamental quarks. Knowledge of the critical physics in these cases may offer clues regarding the critical physics of the more difficult problem of QCD with three colors.

Here, we will consider QCD with two colors. In this case, quark and antiquark states transform similarly under global color rotations. They can be combined into spinors with an extended flavor symmetry SU($2N_f$) for which $\langle qq\rangle$ baryons and $\langle\bar{q}q\rangle$ mesons belong to the same multiplets [10,11]. In particular, the lightest baryons and the pions have a common mass, m_π. This spectrum determines the properties of the ground state for small chemical potential $\mu > 0$. General arguments [12] indicate that a transition from the vacuum to a state with finite baryon density should take place at a critical chemical potential, μ_c, which is the lowest ratio of energy to baryon number that can be realized by an excited state of the system. Here, this state is populated by light $\langle qq\rangle$ baryons, and the transition is thus expected to take place at $\mu_c = m_\pi/2$. The (T, μ) phase diagram of QCD with two colors has been studied previously by Dagotto et al. using a mean-field model of the lattice action [13]. Their results confirm the transition at μ_c. More recently, the smallness of $\mu_c \sim m_\pi/2$ has been exploited in studies of the zero temperature phase transition using chiral perturbation theory extended to the flavor symmetry SU($2N_f$) [14,15]. Many of these model calculations have been verified by recent lattice simulations [16–21].

We have recently constructed a random matrix model of QCD with three colors which permits thermodynamic competition between chiral and diquark condensation [22]. The extension of this model to QCD with two colors is straightforward and constitutes a useful consistency check. The random matrix model respects the global flavor and color symmetries of the QCD interactions and eliminates much of their remaining detailed structure. For two colors, this model offers a qualitatively correct picture of the phase diagram but, at first sight, appears to fail in two respects. First, in it simplest implementation in which only the two lowest Matsubara frequencies are retained, we find an unphysical behavior of the baryon density and the chiral condensate in vacuum. Second, the random matrix interactions saturate for large μ and do not support diquark condensation at arbitrarily high baryon density.

Our primary goal in this study is to examine these difficulties and their relative importance in establishing a reliable picture of the phase diagram. The first difficulty (i.e. the ground state behavior of the baryon density and the chiral condensate) can be resolved by including all quark Matsubara frequencies, which is equivalent to the introduction of proper Fermi occupation factors. For small T, the full frequency sum also modifies the temperature dependence

of the onset chemical potential from a quadratic law with $\mu_c(T) - \mu_c(0) \sim T^2$ to essential singular behavior with $\mu_c(T) - \mu_c(0) \sim \exp(-\Sigma/T)$, where Σ is the vacuum chiral condensate. The remaining phase diagram is qualitatively unchanged. The Matsubara sum is equivalent to a monotonic mapping of the phase diagram of the original random matrix model, a mapping which therefore preserves the topology of the phase structure.

The second difficulty (i.e. the saturation of the interactions at large μ) results from the lack of a true Fermi sea of states in random matrix models. We consider the effects of a proper Fermi sea by studying a microscopic model with an interaction similar to that of the Nambu-Jona-Lasinio (NJL) model. This model naturally exhibits diquark condensation at all densities. It also yields an additional power law correction to the essential singular dependence of $\mu_c(T)$. It will be shown that other deviations from the prediction of the random matrix model arise only in regions where the condensates are weak and thus sensitive to the detailed form of the interaction. Also related to non-universal features of the interactions is the observation that deviations from the results of chiral perturbation theory for μ on the order of μ_c are determined by the form of the interaction on momentum scales substantially larger than μ_c. This is true for both random matrix and NJL models. The sign of these deviations depends on model details and cannot in general be established from first principles.

The remainder of this paper is organized as follows. We review the random matrix model of Refs. [22], extend it to the case of two colors, and discuss its low temperature properties in Sec. II. We analyze the sum over all Matsubara frequencies in Sec. III and study the NJL model in Sec. IV. We discuss the phase diagrams and the condensation fields for each case and present our conclusions in Sec. V.

II. THE RANDOM MATRIX MODEL

We first consider the random matrix model of Refs. [22] in a form appropriate for two colors and two flavors. In this model, the single-quark Lagrangian is represented by a matrix whose block structure reflects the global chiral and color symmetries of QCD. The matrix elements describe the degrees of freedom associated with the background of gluon fields. Aside from the constraints imposed by the prescribed block structure, all matrix elements are independent and chosen at random. An exact solution can be obtained if their distribution is Gaussian. Then, an integration over this distribution produces a partition function of the form

$$Z(\mu, T) = \int d\sigma \; d\Delta \; \exp\left[-N\Omega(\sigma, \Delta)\right], \tag{1}$$

where T is the temperature and μ is the chemical potential. Here, N is proportional to the matrix size and represents the number of low-lying degrees of freedom involved in the phase transition. This number scales with the volume of the physical system, and the thermodynamic limit therefore corresponds to $N \to \infty$. The integrals in Eq. (1) are performed over auxiliary chiral and diquark fields, σ and Δ. We consider here the familiar chiral channel, $\sigma \sim \langle \bar{q}q \rangle$, and the diquark channel, $\Delta \sim \left\langle q\, C\gamma_5\, \tau_2\, \tau_2^F\, q \right\rangle$, where C is the charge conjugation matrix ($C\gamma_\mu C = \gamma_\mu^T$) and where τ_2 and $\tau_2^{\rm F}$ are the antisymmetric SU(2) color and flavor generators [15]. (For a related random matrix model which takes into account additional effects from instanton–anti-instanton molecules, see [23].)

For single-gluon exchange, the thermodynamic potential Ω assumes the form

$$\Omega(\sigma, \Delta) = A(\sigma^2 + \Delta^2) - \mathrm{Tr} \log S(\sigma, \Delta) + \Omega_{\rm reg}, \tag{2}$$

where A characterizes the coupling strengths of the interactions in the chiral and diquark channels. (These strengths are equal for single-gluon exchange.) The quantity $S(\sigma, \Delta)$ is the propagator for a single quark in the background of the condensation fields, σ and Δ. The trace is performed over the quark Matsubara frequencies $\omega_n = i\mu + (2n+1)\pi T$, where n is an integer running from $-\infty$ to ∞.

The random matrix model describes only the thermodynamic contribution from low-energy modes. The effects of the remaining high-energy modes can, in principle, lead to a "regular" term, $\Omega_{\rm reg}$, which does not affect the critical physics. This term is independent of σ and Δ and is an analytic function of T and μ. Although the form of $\Omega_{\rm reg}$ cannot be determined by random matrix arguments, we retain it as a reminder of the presence of high-energy modes. We will later exploit this degree of freedom to adjust the small temperature properties of the model.

In its simplest implementation, the model retains only the two lowest Matsubara frequencies $n = \pm 1$. The trace in Eq. (2) is then reduced to

$$\mathrm{Tr} \log S(\sigma, \Delta) = \sum_{\pm} \log(E_\pm^2(\sigma, \Delta) + \pi^2 T^2), \tag{3}$$

where $E_\pm(\sigma, \Delta)$ represent the quark ($-$) and antiquark ($+$) excitations energies in the background of the condensation fields,

$$E_\pm(\sigma,\Delta) \equiv \left((\sigma + m \pm \mu)^2 + \Delta^2\right)^{1/2}. \tag{4}$$

The simplest model thus consists of Eqs. (2), (3) and (4). We note that a similar form of the potential $\Omega(\sigma,\Delta)$ is also obtained for a chiral random matrix theory with a Dyson index $\beta = 1$ [24], in which one retains only the chiral and diquark channels. In contrast to the present model, this theory makes explicit use of the pseudoreality of QCD with two colors by choosing real matrix elements. However, it does not refer explicitly to color and spin quantum numbers. As a result, the diquark condensate is different from that in the present model and develops instead in the $\langle q^T\gamma_5 q\rangle$ channel. Since the two models possess interactions with similar symmetries among their respective condensates, they naturally lead to similar potentials $\Omega(\sigma,\Delta)$.

Returning to our model, we first consider the chiral limit, $m = 0$. Then, the condensation fields in vacuum ($\mu = T = 0$) appear only in the combination $\sigma^2 + \Delta^2$, and the system obeys the extended flavor symmetry SU(4). The spontaneous formation of a chiral condensate, $\sigma \neq 0$ and $\Delta = 0$, further breaks the symmetry down to Sp(4). A pure chiral solution, $(\sigma,\Delta) = (\Sigma, 0)$, can be transformed into a pure diquark solution, $(\sigma,\Delta) = (0,\Sigma)$, by an SU(4) rotation. These two solutions are thus thermodynamically indistinguishable, and they describe a single phase with $\sigma^2 + \Delta^2 = \Sigma^2 = 2/A$. This phase persists up to a critical temperature $T_c = \Sigma/\pi$ above which all condensation fields vanish and the SU(4) symmetry is restored via a second-order transition. (This is a mean-field result; renormalization group arguments show that for two or more flavors, fluctuations may actually drive the transition first-order [25].) For $T = 0$, a positive chemical potential, $\mu > 0$, breaks the SU(4) symmetry down to $\mathrm{SU_L(2)} \times \mathrm{SU_R(2)} \times \mathrm{U(1)_B}$; a quark mass $m \neq 0$ breaks it further to $\mathrm{SU_V(2)} \times \mathrm{U(1)_B}$ [14,15]. In the following, we consider light quarks by choosing $m \ll \Sigma$, where $\Sigma = \sqrt{2/A}$ is the vacuum chiral condensate for $m = 0$. Note that for $m \neq 0$, the chiral field is no longer a true order parameter, and the second-order phase transition at $\mu = 0$ becomes a cross-over.

The diquark field, Δ, remains a true order parameter even when $m \neq 0$. The system favors the formation of diquark pairs in regions where $\partial^2\Omega/\partial\Delta^2(\sigma,0) < 0$, and a pure chiral solution can be a saddle-point of the potential at best. There is therefore a second-order phase transition along the line $\partial^2\Omega/\partial\Delta^2(\sigma(\mu,T),0) = 0$, where $\sigma(\mu,T)$ obeys the chiral gap equation $\partial\Omega(\sigma,0)/\partial\sigma = 0$. This line is given by the relation

$$\mu^2 + \pi^2 T^2 = \frac{\Sigma^2\mu^2}{\mu^2 - m^2} - \frac{\Sigma^4 m^2}{4(\mu^2 - m^2)^2} \tag{5}$$

and delimits a region in the (T,μ) plane as illustrated in Fig. 1 (a). (We will discuss Figs. 1 (b) and (c) below.) Its intercept with the $T = 0$ axis determines the onset chemical potential

$$\mu_c^2 = \frac{m\Sigma}{2} + \mathcal{O}(m^2), \tag{6}$$

which becomes $\mu_c(T) \sim \mu_c(1 + \pi^2T^2/(4\Sigma^2))$ for small T. According to the arguments in the introduction, the onset chemical potential of Eq. (6) also obeys $\mu_c = m_\pi/2$. This leads us to identify the pion mass as $m_\pi \simeq m^{1/2}\Sigma^{1/2} + \mathcal{O}(m)$.

This result is not trivial and may be regarded as the random matrix analogue of the current-algebra relation $m_\pi \sim m^{1/2}$. To understand the origin of this relation in the present model, consider the random matrix vacuum. For simplicity, assume one quark flavor and ignore diquark condensation by setting $\Delta = 0$. Consider first $m = 0$. In this case, we know that the spontaneous breaking of chiral symmetry guarantees the existence of a massless Goldstone mode [26] independent of the number of colors [27]. Consider next the case of a finite but small mass m, for which chiral symmetry is explicitly broken. The previous Goldstone mode now describes the lowest-lying fluctuations around the global minimum of $\Omega(\sigma,0)$, which is given by $\sigma_0 = \Sigma - m/2 + \mathcal{O}(m^2/\Sigma)$. From Eqs. (2), (3), and (4) with $\Delta = 0$, we find that the energy of fluctuations around this solution is given as

$$\Omega_{\mathrm{fluct}} \simeq \frac{2}{\Sigma^2}\left((\sigma_0 + \delta\sigma)^2 + \delta\pi^2\right) - 2\log\left[(\sigma_0 + m + \delta\sigma)^2 + \delta\pi^2\right], \tag{7}$$

where the pion mode $\delta\pi$ describes oscillations in the direction with $\langle\bar{q}\gamma_5 q\rangle \neq 0$ and $\delta\sigma$ describes those in the $\langle\bar{q}q\rangle$ direction. Thus the mass, m, acts as an external field with an almost linear coupling to the order parameter; for small m, the symmetry breaking term goes as $\delta\Omega_{\mathrm{fluct}} \propto -m\,\sigma_0$. This coupling causes the curvature of the free-energy in the soft direction to be proportional to m. Expanding to second order in $\delta\sigma$ and $\delta\pi$ and working to lowest order in m/Σ, we find

$$\Omega_{\mathrm{fluct}} \simeq \Omega|_{\delta\sigma=\delta\pi=0} + \frac{4}{\Sigma^2}\,\delta\sigma^2 + \frac{2m}{\Sigma^3}\,\delta\pi^2 + \cdots \tag{8}$$

This allows us to identify the mass ratio m_π^2/m_σ^2 as $\sim m/\Sigma$ and deduce $m_\pi^2 \sim m$, which confirms the result of Eq. (6). The generalization of this argument to include fluctuations in the $\langle qq\rangle$ channel is straightforward and leads to results

similar to those of chiral perturbation theory for the constant terms [15]. (Random matrix theory cannot reproduce terms with spatial derivatives.)

We now return to the diquark condensed phase. The two gap equations, $\partial\Omega/\partial\sigma = 0$ and $\partial\Omega/\partial\Delta = 0$, possess a single solution with both $\sigma \neq 0$ and $\Delta \neq 0$,

$$\sigma = -m + \frac{\Sigma^2}{2}\frac{m}{\mu^2 - m^2}, \tag{9}$$

$$\sigma^2 + \Delta^2 = \Sigma^2 + m^2 - \mu^2 - \pi^2 T^2, \tag{10}$$

where $\Sigma \equiv (2/A)^{1/2}$. Expanding to the lowest orders in m/Σ, the fields near the condensation edge $\mu \approx \mu_c$ obey

$$\sigma \simeq \Sigma\,\frac{\mu_c^2}{\mu^2} - m + \mathcal{O}\left(\frac{m^2}{\Sigma}\right), \tag{11}$$

$$\sigma^2 + \Delta^2 = \Sigma^2 - \pi^2 T^2 + \mathcal{O}(m\Sigma). \tag{12}$$

For $T = 0$ and to leading order in m/Σ, these results coincide with chiral perturbation theory [15]. For $\mu > \mu_c$, the chiral field decreases like $1/\mu^2$, and this saddle-point solution rotates into a pure diquark solution keeping $\sigma^2 + \Delta^2$ nearly constant. Corrections of order $m\Sigma$ in Eq. (12) depend on the explicit functional form of the potential of Eq. (2) (i.e. here, a logarithm involving certain combinations of σ and Δ) and are thus not universal. We will see below examples of other functional dependences which give different corrections in $m\Sigma$. If we now turn to the non-condensed phase ($\mu < \mu_c$ and $\Delta = 0$), we find

$$\sigma \simeq \Sigma - \frac{m}{2} + \frac{\mu^2 - \pi^2 T^2}{2\Sigma} + \mathcal{O}\left(\frac{m^2}{\Sigma}\right), \tag{13}$$

where terms of order m and higher are again not universal.

Although the results to lowest order in m/Σ are consistent with our expectations, higher-order terms give rise to certain unphysical properties. For $T = 0$ and $\mu < \mu_c$, we expect that, in the absence of confinement, the lowest-lying excitations carrying a net baryon number are single quarks with an energy $\sim \Sigma$. Below the condensation edge, we have $\mu < \mu_c \ll \Sigma$, and the excitation energy $\sim \Sigma$ is well above the Fermi level μ. The ground state should thus have a chiral field equal to its value at $\mu = 0$ and a baryon density of zero. We find instead a chiral field $\sigma \simeq \Sigma - m/2 + \mu^2/(2\Sigma)$, which increases quadratically with μ. The behavior of the baryon density, $n_{\rm B} \equiv -\partial\Omega/\partial\mu$, is also incorrect. From the solutions above, we find that the potential in each phase obeys

$$\Omega \simeq \Omega_{\rm vac} - \frac{4m}{\Sigma} + 2\,\frac{\mu^2 - \pi^2 T^2}{\Sigma^2} + \Omega_{\rm reg} + \mathcal{O}\left(\frac{m^2}{\Sigma^2}\right) \quad (\mu < \mu_c), \tag{14}$$

$$\Omega \simeq \Omega_{\rm vac} - \frac{m^2}{\mu^2} - 2\,\frac{\mu^2 + \pi^2 T^2}{\Sigma^2} + \Omega_{\rm reg} + \mathcal{O}\left(\frac{m^2}{\Sigma^2}\right) \quad (\mu \gtrsim \mu_c), \tag{15}$$

where the vacuum energy is $\Omega_{\rm vac} = 2 - 2\log\Sigma^2$. These relations lead to negative baryon density for $\mu < \mu_c$!

This behavior is a result of having truncated the Matsubara sum in Eq. (2) to the two lowest frequencies. This approximation does not affect the critical physics but does modify bulk properties. It is therefore appropriate to correct the shortcomings of such an approximation naturally with an appropriate adjustment of the regular term, $\Omega_{\rm reg}$, in the thermodynamic potential of Eq. (2). The requirement that the baryon density should vanish for $\mu < \mu_c$ is readily met by the choice $\Omega_{\rm reg} = -2\mu^2/\Sigma^2$. For $T = 0$, we then obtain a baryon density of

$$n_{\rm B} = -\frac{\partial\Omega}{\partial\mu} = \begin{cases} 0 + \mathcal{O}\left(\frac{m}{\Sigma^2}\right) & (\mu < \mu_c) \\ 8\mu/\Sigma^2\left(1 - \mu_c^4/\mu^4\right) + \mathcal{O}\left(\frac{m}{\Sigma^2}\right) & (\mu > \mu_c)\,, \end{cases} \tag{16}$$

which has the same μ-dependence as that found in chiral perturbation theory [15]. The terms of order $\mathcal{O}(m/\Sigma^2)$ are positive, hence $n_{\rm B} > 0$ for all μ.

To summarize, the random matrix model reproduces the results of chiral perturbation theory to leading order in m/Σ for the condensation fields and for the baryon density, provided only that we exploit the freedom of including a component $\Omega_{\rm reg}$ in the thermodynamic potential. This addition cannot, however, affect the condensation fields, and σ still grows weakly with μ below the condensation edge. The variation of the condensation fields near the edge is shown in Fig. 2 (*a*). (Figs. 2 (*b*) and (*c*) will be discussed below.) It is, in fact, difficult to discern the dependence of σ on μ for $\mu < \mu_c$ as the quadratic term $\sim \mu^2/\Sigma$ is of order m/Σ relative to the leading term, which is of order $\sim \Sigma$. Figure 3 (*a*) shows the condensation fields for selected temperatures.

III. SUMMING OVER ALL MATSUBARA FREQUENCIES

The μ-dependence of σ and $n_{\rm B}$ found in the preceeding section was obtained by retaining only the lowest Matsubara frequencies. Although this approximation is reasonable for the study of the finite temperature phase diagram of QCD with three colors, it is bound to break down in the present case for small temperatures near the condensation edge. As T becomes smaller, adjacent Matsubara frequencies $\pm 3\pi T$, $\pm 5\pi T$, ... come closer to those retained and eventually form a continuum as $T \to 0$. In physical terms, the frequency continuum at $T = 0$ enforces the exclusion principle by introducing Fermi occupation factors.

As shown in the Appendix, the sum over all Matsubara frequencies leads to a partition function of the form

$$Z(\mu, T) = \int d\sigma \, d\Delta \, \exp\{-N\beta\Omega(\sigma, \Delta)\} \tag{17}$$

where $\beta \equiv 1/T$. The thermodynamic potential is now given by

$$\Omega(\sigma, \Delta) = \frac{\sigma^2 + \Delta^2}{\Sigma} - \sum_{\pm} \Big\{ E_{\pm}(\sigma, \Delta) + 2T \log[1 + \exp\{-\beta E_{\pm}(\sigma, \Delta)\}] \Big\} + \tilde{\Omega}_{\rm reg} \, . \tag{18}$$

The excitation energies, $E_{\pm}(\sigma, \Delta)$, are given by Eq. (4). As before, we allow for the inclusion of a term $\tilde{\Omega}_{\rm reg}$, analytic in μ and T, which represents the contribution from high-energy modes. The requirement that the $T = \mu = 0$ vacuum has zero baryon density is met by taking $\tilde{\Omega}_{\rm reg}$ as a constant. This constant is further set to $\tilde{\Omega}_{\rm reg} = -\Sigma - 2m$, in order for the vacuum to have zero pressure. Again, Σ is the chiral field for $T = \mu = m = 0$.

Compared to the previous random matrix model, the full Matsubara sum has introduced Fermi occupation factors, $f(x) = \{1 + \exp(x/T)\}^{-1}$. This is easily seen in the two gap equations

$$2\,\frac{\sigma}{\Sigma} = \sum_{\pm} \frac{\sigma + m \pm \mu}{E_{\pm}(\sigma, \Delta)} \, (1 - 2f[E_{\pm}(\sigma, \Delta)]) \tag{19}$$

$$2\,\frac{\Delta}{\Sigma} = \sum_{\pm} \frac{\Delta}{E_{\pm}(\sigma, \Delta)} \, (1 - 2f[E_{\pm}(\sigma, \Delta)]) \, . \tag{20}$$

In this form, the gap equations possess solutions which, at $T = 0$ and for all μ below the condensation edge, exhibit the same properties as those of the vacuum, $\mu = T = 0$. For $\mu < \mu_c$, we now find a pure chiral solution with $\Delta = 0$ and a constant chiral field $\sigma = \Sigma$. The baryon density vanishes exactly. The onset chemical potential, μ_c, at $T = 0$ is determined by requiring that both gap equations are satisfied while taking $\Delta \to 0^+$. We find $\mu_c = (m(\Sigma + m))^{1/2} \simeq (m\Sigma)^{1/2} + \mathcal{O}(m)$. For $\mu \gtrsim \mu_c$, the gap equations possess a single solution which reproduces the result of chiral perturbation theory to lowest order in m/Σ. Higher-order terms depend on the functional form of Eq. (18) and are different from those obtained in Eqs. (9) and (10). These terms are therefore not universal. We show the fields σ and Δ near the condensation edge in Fig. 2(b). Figure 3(b) presents their behavior as a function of μ for selected temperatures.

The phase diagram in the full (T, μ) plane, shown in Fig. 1(b), appears as a mere remapping of the diagram of Fig. 1(a). Both diagrams have the same topology. The most dramatic effect of this remapping is a sharp vertical stretching of the condensation edges at low and high chemical potentials. We show in the Appendix that, at the lower edge, the previous behavior of $\mu_c(T) - \mu_c(0) \sim T^2$ is now replaced by essential singular behavior with $\mu_c(T) - \mu_c(0) \sim \exp[-(\Sigma + m)/T] \sinh[\mu_c(0)/T]$. This behavior is clearly a consequence of the introduction of Fermi occupation factors. These factors automatically imply detailed balance, whereby two single-quark states separated by an energy difference ΔE are weighted by a relative factor of $\exp(-\Delta E/T)$. Except for these modifications at low temperature, the global picture remains remarkably similar to that of Fig. 1(a).

IV. BUILDING A FERMI SEA

Cooper pairing occurs in any attractive channel independent of its interaction strength. Thus, even though the QCD interactions weaken on the momentum scales appropriate for large densities, the existence of a diquark phase at mean field level should naturally continue to arbitrarily high μ. For three colors, model calculations with large μ and small coupling constant, g, find a pairing gap $\Delta \sim \mu g^{-5} \exp(-{\rm c}/g)$ where c is a constant [28]. Similar behavior is to be anticipated in QCD with two colors.

By contrast, the random matrix interactions saturate at large μ and do not support diquark gaps at arbitrarily high density. This weakening of $\langle qq \rangle$ correlations is ultimately related to the absence of a Fermi surface. The quark states in the random matrix model do not carry a momentum, and there is therefore no Fermi sea. In fact, for fixed σ and Δ, the system has only two energy levels (the $E_\pm(\sigma, \Delta)$ in Eq. (4)), whereas a microscopic model exhibits a continuum of states labeled by their particle momenta.

In this section, we study the effects of a true Fermi sea on the global picture established above and consider a microscopic theory with an interaction suggested by the Nambu-Jona-Lasinio model [29]. The structure of the interaction for large momenta must be specified by an appropriate form factor. A sharp three-momentum cutoff saturates the interactions at large momenta and does not lead to a diquark gap for all μ. Since we wish to explore a model which supports pairing at all densities, we choose instead a soft form factor,

$$\mathcal{F}(q) = \frac{1}{1 + (q/\Lambda)^2}\,, \tag{21}$$

which weakens the interactions with a scale of $q \sim \Lambda$. This choice leads to a model similar to that adopted by Berges and Rajagopal in their study of diquark condensation for $N_c = 3$ [30]. Our intent is to investigate general trends, and we are not concerned with precise parameter values. Thus, we take $\Lambda = 3\Sigma$, where Σ is again the chiral field in vacuum for $m = 0$. The mass, m, is chosen as $m = 0.01\,\Sigma$ in order to have a clear separation between the three scales m, $\sqrt{m\Sigma}$, and Σ. (We have explored other ranges of parameters and found the same basic trends.) The introduction of momentum dependence transforms the model of Eq. (18) into

$$\Omega = A(\sigma^2 + \Delta^2) - \frac{2}{\pi^2} \sum_{\pm} \int_0^\infty dq\; q^2 \; \Big\{ E_\pm(q, \sigma, \Delta) + 2T \log\left(1 + \exp\left\{-\beta E_\pm(q, \sigma, \Delta)\right\}\right) \Big\}, \tag{22}$$

where the excitations energies are now momentum dependent,

$$E_\pm(q, \sigma, \Delta) = \left((E(q) \pm \mu)^2 + \mathcal{F}^4(q)\Delta^2\right)^{1/2}, \tag{23}$$

with $E(q) = (q^2 + (m + \sigma\mathcal{F}^2(q))^2)^{1/2}$. As before, the coupling constant A is fixed by requiring that the vacuum chiral field be equal to $\sigma = \Sigma$ for $m = 0$.

The system now naturally supports a diquark condensate at all densities. To illustrate the mechanism at work, consider first the chiral limit $m = 0$. Then, for $T = 0$ and $\mu > 0$, we find that $\sigma = 0$ while Δ obeys the gap equation

$$A = \frac{1}{\pi^2} \int_0^\infty dq\, q^2 \sum_{\pm} \mathcal{F}(q)^4 \frac{1}{\sqrt{(q \pm \mu)^2 + \mathcal{F}(q)^4\Delta^2}}. \tag{24}$$

When $\Delta = 0$, the right side of this equation diverges logarithmically due to the behavior of the integrand for q near μ; it vanishes for large Δ. Hence for $A > 0$, the equation always has a solution with $\Delta > 0$. For small μ, Δ is sufficiently large that the logarithmic singularity for $q \sim \mu$ is inoperative. The range of contributing momenta is then determined by the form factor $\mathcal{F}(q)$ and includes all $q < \Lambda$. As μ increases, the momentum window in which the integrand is logarithmically large, $|q - \mu| \sim \Delta\mathcal{F}^2(\mu)$, decreases due to the form factor, and the strength of the logarithmic singularity increases. It eventually dominates the integral at large μ and leads to exponentially small gaps which decrease like $\Delta(\mu) \propto \exp[-A/(\mu^2\mathcal{F}(\mu)^4)]$.

A similar mechanism is encountered when we depart from the chiral limit. For $m > 0$, we have $\sigma \neq 0$, and the condensation fields are given by the solution of two coupled gap equations. These equations again exhibit a logarithmic divergence as $\Delta \to 0$ for momenta q satisfying $E(q) \simeq \mu$, where $E(q) = (q^2 + (m + \sigma F(q)^2)^2)^{1/2}$. We have $E(q) \gtrsim m + \sigma$, where the chiral field is of order $\sigma \sim \Sigma$ for $\mu \sim \mu_c$ and decreases for larger μ. Hence, the condition $E(q) \sim \mu$ is not obeyed for small μ as $E(q) \sim \Sigma$ when $\mu \to 0$. It is, however, satisfied starting at some μ in the range $\mu_c < \mu < \Sigma$ where σ decreases below Σ. For large μ, the singularity condition can always be met. Therefore, for $T = 0$ and $\mu \gtrsim \Sigma$, the logarithmic singularity is active and dominates the momentum integral. It follows that Δ is always non-vanishing for moderate and large μ and that the diquark phase persists for all large μ as shown in Fig. 1(c).

Figure 3(c) shows the condensation fields for various fixed T. As we have just argued, the maximum diquark field, and therefore also the critical temperature, decrease exponentially with μ when $\mu \gtrsim \Lambda$. In this region, the thermodynamic potential is dominated by large momenta and is very sensitive to form factors. This situtation stands in contrast to the three color case [30], which has different coupling constants and exhibits a different evolution of the diquark field. There, most of the interesting variations in $\Delta(\mu)$ and in the phase transition line take place below the cutoff, $\mu < \Lambda$. These results are likely to be much less sensitive to form factor effects.

Returning to the problem at hand, it is useful to remember that the present models have been implemented at mean-field level. Results in regions where condensation fields are weak cannot be regarded as reliable since weak condensates may not survive fluctuations. An illustrative example of the effects of long-wavelength fluctuations has recently been considered in lattice studies of the NJL model in two dimensions. There, the data suggests a strong suppression of the diquark order parameter with respect to the mean-field predictions and also provides indications of strong critical fluctuations [31].

Results for small μ are more reliable. The critical physics near the condensation edge, μ_c, is primarily determined by symmetries and is most likely protected by them. For the NJL model, we find results which are remarkably similar to those of the previous sections. For zero T, we find a second-order phase transition from a chiral phase to a diquark phase at a critical chemical potential $\mu_c \sim m^{1/2}$. The chiral field is constant for $T = 0$ and $\mu < \mu_c$ and decreases roughly like $1/\mu^2$ for $\mu > \mu_c$. The diquark field and the baryon density increase in this region. For $T = 0$ and near the condensation edge, the fields follow chiral perturbation theory as illustrated in Fig. 2 (c). For small T, the critical chemical potential behaves as $\mu_c(T) - \mu_c(0) \sim T^{3/2} \exp\{-\Sigma/T\} \sinh[\mu_c(0)/T]$. The exponent 3/2 in the power law correction is directly related to the dimension of the momentum integrals in Eq. (22).

V. CONCLUDING REMARKS

The two random matrix models and the NJL model considered here all reproduce the predictions of chiral perturbation theory in the vicinity of $T = 0$ and near the condensation edge, $\mu = \mu_c$, but each of these models contains additional, non-universal corrections. These corrections can, in part, be attributed to the effects of momentum scales larger than m_π.

This can be seen by considering both chiral limit and departures from it. In the strict chiral limit, $m = 0$, the condensation edge goes to $\mu_c = 0$, and much of the critical structure which we have previously discussed disappears. The chiral field vanishes for all $\mu > 0$, and a finite diquark field develops for T below a critical temperature $T_c(\mu)$. Variations in $\Delta(\mu)$ as a function of μ occur on a large and model-dependent scale. Away from the chiral limit, we can distinguish two regions. First, in the vicinity of the condensation edge, all thermodynamic quantities follow the predictions of chiral perturbation theory and vary with μ on a scale $\mu_c \sim m_\pi$. Second, far from the condensation edge, the thermodynamic properties of all three models vary on the much larger scales encountered in the chiral limit. In fact, for $\mu \gg \mu_c$ the condensation fields differ from those for $m = 0$ by powers of m. The scale $m_\pi \sim m^{1/2}$, which is central to chiral perturbation theory, thus no longer plays a role in this region where larger and non-universal scales are dominant.

The resulting picture for $\mu \gg \mu_c$ found for each of the models considered here is thus quite different from that predicted by chiral perturbation theory. For the random matrix models, the relevant scale of variation is the vacuum chiral field Σ, which is intimately related to the variance of the matrix elements. This is also the scale on which $\langle qq \rangle$ correlations weaken. The saturation of the interactions manifests itself in a decrease of $\Delta(\mu)$ with μ in both random matrix models, compare Figs. 2 (a) and (b). By contrast, the dominant scale of variation for $\mu \gg \mu_c$ in the NJL model is the momentum cutoff, Λ. This scales acts in a different way. Because of the logarithmic singularity in the gap equations discussed above, $\Delta(\mu)$ increases until $\mu \sim \Lambda$. For larger values of μ, interactions weaken due to the form factors, and Δ decreases with μ. The logarithmic singularity also causes the baryon density to rise as μ increases from μ_c. For the NJL model, deviations from the results of chiral perturbation theory are opposite to those of the random matrix models as shown in Fig. 1(c).

The lesson is that large momentum scales tend to play a dominant role away from the condensation edge. This should be kept in mind when interpreting lattice data. In this regard, it is interesting to note that the lattice mean-field action of Dagotto et al. [13] leads to a phase diagram with a second-order line which terminates at some high μ and $T = 0$ in a manner similar to the phase diagrams in Figs. 1(b) and (c). This ending of the transition line is attributed in Ref. [18] to a saturation of the lattice interactions.

A final comment concerns the evolution of the baryon density as a function of μ. We have not displayed baryon densities for $\mu \gg \mu_c$ because random matrix models describe only the contribution of soft modes. Since the baryon density receives contributions from both high- and low-energy modes, its behavior can be quite different from the predictions of random matrix models. Similarly, baryon densities calculated with the NJL model are sensitive both to the form factor chosen and to variations in the quark mass m over much of the phase diagram. Again, this suggests that such results should be considered with care. By contrast, we have demonstrated that thermodynamic properties near the condensation edge are dominated by symmetries and that the models considered provide a qualitatively correct description of the baryon density in this region.

In conclusion, we have found that a random matrix model which retains only two Matsubara frequencies correctly reproduces the leading-order results of chiral perturbation theory. Beyond leading order, however, it produces certain

unphysical results including negative baryon densities for small μ and a chiral condensate which varies with μ. These pathologies can be eliminated by the inclusion of all Matsubara frequencies. This extension of the random matrix model also correctly produces an essential singularity in the second-order line at $T = 0$. Neither variant of the random matrix model considered here can support diquark condensation at arbitrarily high baryon density since neither contains a true Fermi sea of states. A microscopic model capable of supporting diquark condensation at all densities does so at the cost of introducing significant model dependence. Near the condensation edge, a three dimensional model also induces power law corrections to the temperature dependence of the onset chemical potential. This result is robust.

The present random matrix models contain the ingredients necessary to produce the correct critical physics near the condensation edge. All thermodynamic quantities in this region are dominated by those symmetries which we have implemented in the interactions. Given only a minor and physically reasonable adjustment in the treatment of the Matsubara sum, the model reproduces the results of chiral perturbation theory or of any other microscopic model which implements the same symmetries. Away from the condensation edge, however, the random matrix interactions saturate and lead to non-physical results. It seems unlikely that "improvements" of the theory in this region, whether in the form of an extended random matrix model or of a detailed microscopic model, will be beneficial. The large μ region is not dominated by symmetries, and results in that region will unavoidably be fragile and model dependent. Since the random matrix approach is by construction free of the inevitable details of more microscopic models, it provides a simple and useful way of distinguishing between those results which are dominantly influenced by symmetries and those which are not.

ACKNOWLEDGEMENTS

We thank D. Toublan, J. J. M. Verbaarschot, and A. Schäfer for stimulating discussions and K. Splittorff for his critical reading of the manuscript. We also thank the DOE Institute for Nuclear Theory at the University of Washington for its hospitality and the Department of Energy for partial support during the early stages of this work.

APPENDIX

A. Sum over all Matsubara frequencies

Here we consider certain technical details of the random matrix model in which all Matsubara frequencies are included. Following Ref. [32], we introduce a Euclidean time which is the Fourier conjugate of the Matsubara frequency and which runs from $0 \leq t \leq \beta \equiv 1/T$.

Consider first the logarithmic term in $\Omega(\sigma, \Delta)$, Eq. (2), whose frequency trace is

$$\mathrm{Tr}\log S(\sigma,\Delta) = \sum_{\pm}\sum_{n=-\infty}^{\infty} \log[\beta^2\left((2n+1)^2\pi^2T^2 + \Delta^2 + (\sigma + m \pm \mu)^2\right)] \; . \tag{25}$$

Here, we have included a piece of the term $\Omega_{\rm reg}$ from Eq. (2) by inserting the prefactor $\beta^2 = T^{-2}$ in order to ensure that the argument of the logarithm is dimensionless. The sum over n on the right side of this equation is best evaluated by taking the derivative of $\mathrm{Tr}\log S$ with respect to either σ or Δ. Using then the summation formula

$$\tanh[x] = \sum_{n=-\infty}^{\infty} \frac{x}{x^2 + (n+1/2)^2\pi^2}, \tag{26}$$

and integrating back over the condensation fields, we arrive at the result

$$\mathrm{Tr}\log S(\sigma,\Delta) = \beta\sum_{\pm}\{E_{\pm}(\sigma,\Delta) + 2T\log[1+\exp[-\beta E_{\pm}(\sigma,\Delta)]]\} + c(\mu,T). \tag{27}$$

Here, c is independent of σ and Δ and the $E_{\pm}(\sigma,\Delta)$ are the single-quark energies of Eq. (4).

The frequency sum over the quadratic terms is simpler. Since the condensation fields are constant in time, Fourier transformation to Euclidean time gives

$$\mathrm{Tr}A(\sigma^2+\Delta^2) = \int_0^{\beta} dt A\left(\sigma^2+\Delta^2\right) = \beta A(\sigma^2+\Delta^2). \tag{28}$$

The saddle-point effective potential is the sum of Eqs. (27) and (28) plus an additional regular piece, $\beta\tilde{\Omega}_{\rm reg}$, which includes $c(\mu,T)$ and is chosen as follows. We wish to obtain a $T=\mu=0$ vacuum to have zero baryon density. This constraint is met by taking $\tilde{\Omega}_{\rm reg}$ as a constant. The additional requirement that the $T=\mu=0$ vacuum should have zero pressure sets $\tilde{\Omega}_{\rm reg}=-\Sigma-2m$, where Σ is the vacuum chiral field. Since we are primarily concerned with the functional form of the effective thermodynamic potential, we have chosen to tune A to $A=1/\Sigma$ in order to obtain a chiral field $\sigma=\Sigma$ in vacuum. This choice simplifies comparison with the other models. Removing a common prefactor β, we arrive at Eqs. (17) and (18).

B. Temperature dependence of the onset chemical potential

In this section, we determine the temperature dependence of the onset chemical potential, $\mu_c(T)$, for both the random matrix model with all Matsubara frequencies included and the NJL model. We first illustrate the derivation for the simple random matrix model. For fixed T, the onset chemical potential satisfies the chiral and the diquark gap equations with Δ set to zero. From $\Omega(\sigma,\Delta)$ in Eq. (18), we have

$$\frac{2}{\Sigma}\,\sigma=\tanh[\frac{\sigma+m+\mu}{2T}]+\tanh[\frac{\sigma+m-\mu}{2T}], \tag{29}$$

$$\frac{2}{\Sigma}\;=(\sigma+m+\mu)^{-1}\tanh[\frac{\sigma+m+\mu}{2T}]+(\sigma+m-\mu)^{-1}\tanh[\frac{\sigma+m-\mu}{2T}]. \tag{30}$$

The small T behavior can be obtained by expanding the chiral field and the chemical potential around their values at $T=0$ and $\mu=\mu_c$ (i.e. $\sigma=\Sigma+\delta\sigma$ and $\mu=\mu_c+\delta\mu$) and expanding the explicit temperature dependence as $\tanh[x/(2T)]\simeq 1-2\exp[-x/T]$. To first order, this expansion gives

$$2\frac{\delta\sigma}{\Sigma}\simeq -4\exp[-(\sigma+m)/T]\cosh[\mu_c/T], \tag{31}$$

$$\begin{aligned}0\simeq\;&-\delta\sigma\left\{\frac{1}{(\Sigma+m+\mu_c)^2}+\frac{1}{(\Sigma+m-\mu_c)^2}\right\}-\\&\delta\mu\left\{\frac{1}{(\Sigma+m+\mu_c)^2}-\frac{1}{(\Sigma+m-\mu_c)^2}\right\}-\\&2\exp[-(\Sigma+m)/T]\left\{\frac{\exp[-\mu_c/T]}{\Sigma+m+\mu_c}+\frac{\exp[\mu_c/T]}{\Sigma+m-\mu_c}\right\}.\end{aligned} \tag{32}$$

Inserting the first of these relations into the second and expanding the denominators to first order in $\mu_c\sim m^{1/2}$ and zeroth order in m, we obtain the result given in the text:

$$\delta\mu\simeq\Sigma\,\exp[-\frac{\Sigma}{T}]\sinh[\frac{\mu_c}{T}]. \tag{33}$$

Due to the sensitivity of the NJL model to both the mass m and the cutoff parameter Λ, it is more difficult to obtain an exact relationship for $\mu_c(T)$ in this case. We can, however, get a rough estimate by following the previous steps and restricting our attention to terms of zeroth order in m/Σ and first order in μ_c/Σ. An expansion of the two gap equations to these orders then gives

$$\delta\mu\simeq c\sinh[\frac{\mu_c}{T}]\int_0^\infty dq\,q^2\frac{\mathcal{F}(q)^4}{E(q)^2}\exp[-E(q)/T]\,, \tag{34}$$

where c is the constant $c=(\int_0^\infty dq\,q^2\mathcal{F}(q)^4/E(q)^3)^{-1}$ and $E(q)=(q^2+\Sigma^2\mathcal{F}(q)^4)^{1/2}$ is the single-quark energy for $\Delta=0$ and $m=0$. For $T\to 0$, the integral on the right side can safely be approximated by saddle-point methods. Expanding $E(q)$ as $\Sigma+q^2(1-4\Sigma^2/\Lambda^2)/(2\Sigma)$ and setting $q=0$ in the denominator, we obtain

$$\delta\mu\simeq c\sqrt{\frac{\pi}{2}}\,\sinh[\frac{\mu_c}{T}]\,\left(\frac{T}{\Sigma}\right)^{3/2}\,\frac{\Sigma\exp[-\Sigma/T]}{(1-4\frac{\Sigma^2}{\Lambda^2})^{3/2}}. \tag{35}$$

Comparison with Eq. (33) reveals an additional power-law correction of $T^{3/2}$. This correction is a consequence of having a genuine continuum of momentum states; the exponent 3/2 is half the dimensionality of the space.

[1] B. Barrois, Nucl. Phys. **B129**, 390 (1977); D. Bailin and A. Love, Phys. Rept. **107**, 325 (1984).
[2] R. Rapp, T. Schäfer, E. V. Shuryak, and M. Velkovsky, Phys. Rev. Lett. **81**, 53 (1998); Ann. of Phys. **280**, 35 (2000).
[3] M. Alford, K. Rajagopal, and F. Wilczek, Phys. Lett. B **422**, 247 (1998).
[4] For a review, see K. Rajagopal and F. Wilczek, hep-ph/0011333.
[5] D. Blaschke, T. Klähn, and D. N. Voskresensky, Astrophys. J. **533**, 406 (2000); D. Blaschke, H. Grigorian, and D. N. Voskresensky, astro-ph/0009120;
[6] D. Page, M. Prakash, J. M. Lattimer, and A. Steiner, Phys. Rev. Lett. **85**, 2048 (2000).
[7] G. W. Carter and S. Reddy, Phys. Rev. **D62**, 103002 (2000).
[8] M. Alford, J. Berges, and K. Rajagopal, Nucl. Phys. **B571**, 269 (2000).
[9] See for instance the proceedings of *QCD at finite baryon density*, Bielefeld, April 1998, F. Karsh and M.-P. Lombardo, eds., Nucl. Phys. **A642** (1998).
[10] D. Diakonov and V. Petrov, in *Quark Cluster Dynamics*, Lecture Notes in Physics, edited by K. Goeke, P. Kroll, and H. Petry (Springer-Verlag, Berlin, 1992) p. 288.
[11] A. Smilga and J. J. M. Verbaarschot, Phys. Rev. **D51**, 829 (1995).
[12] M. A. Halasz, A. D. Jackson, R. E. Schrock, M. A. Stephanov, and J. J. M. Verbaarschot, Phys. Rev. D **58**, 096007 (1998).
[13] E. Dagotto, F. Karsh, and A. Moreo, Phys. Lett. B **169**, 421 (1986); E. Dagotto and A. Moreo, Phys. Lett. B **186**, 395 (1987).
[14] J. B. Kogut, M. A. Stephanov, and D. Toublan, Phys. Lett. **B464**, 183 (1999).
[15] J. B. Kogut, M. A. Stephanov, D. Toublan, J. J. M. Verbaarschot, and A. Zhitnitsky, Nucl. Phys. **B582**, 477 (2000).
[16] S. Hands, I. Montvay, S. Morrison, M. Oevers, L. Scorzato, and J. Skullerud, Eur. Phys. J. **C17**,285 (2000); S.J. Hands, J. B. Kogut, S. E. Morrison, and D. K. Sinclair, hep-lat/0010028.
[17] For related problems in the case of a finite isospin density, see K. Splittorff, D. T. Son, and M. A. Stephanov, hep-ph/0012274.
[18] R. Aloisio, A. Galante, V. Azcoiti, G. Di Carlo, and A. F. Grillo, hep-lat/0007018; Phys. Lett. **B493**, 189 (2000); hep-lat/0011079.
[19] S. Muroya, A. Nakamura, and C. Nonaka, hep-lat/0010073.
[20] See also B. Allés, M. D'Elia, M.-P. Lombardo, M. Pepe, hep-lat/0010068; E. Bittner, M.-P. Lombardo, H. Markum, and R. Pullirsch, hep-lat/0010018; M. B. Hecht, C. D. Roberts, and S. M. Schmidt, nucl-th/0012023.
[21] M.-P. Lombardo, hep-lat/9907025.
[22] B. Vanderheyden and A. D. Jackson, Phys. Rev. D **61**, 076004 (2000); Phys. Rev. **D62**, 094010 (2000).
[23] S. Pépin and A. Schäfer, hep-ph/0010225.
[24] E. V. Shuryak and J. J. M. Verbaarschot, Nucl. Phys. **A560**, 306 (1993);J. J. M. Verbaarschot, Phys. Rev. Lett. **72**, 2531 (1994); Phys. Lett. B **329**, 351 (1994).
[25] J. Wirstam, Phys. Rev. D **62**, 045012 (2000).
[26] G. W. Carter and A. D. Jackson, Phys. Rev. D **61**, 077902 (2000).
[27] In the context of Ref. [26], this means that the existence of a pole in the current-current correlator does not depend on whether the Dyson index β is one (two colors), or two (three colors).
[28] D. T. Son, Phys. Rev. D **59**, 094019 (1999).
[29] Y. Nambu and G. Jona-Lasinio, Phys. Rev. **122**, 345 (1961).
[30] J. Berges and K. Rajagopal, Nucl. Phys. **B538**, 215 (1999).
[31] S. Hands, B. Lucini, and S. Morrison, hep-lat/0008027.
[32] R. A. Janik, M. A. Nowak, G. Papp, and I. Zahed, Nucl. Phys. **A642**, 191 (1998).

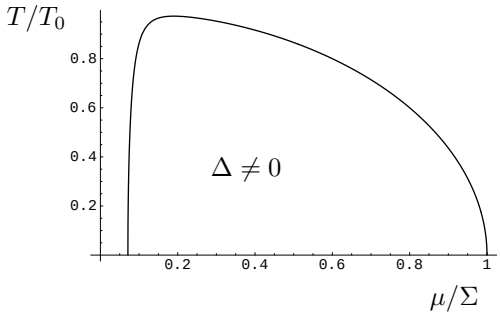

(a)

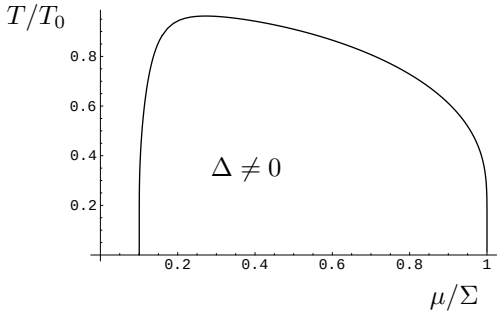

(b)

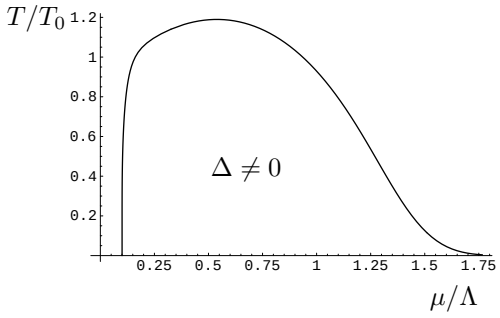

(c)

FIG. 1. Phase diagrams in the (T, μ) plane for the random matrix model with two Matsubara frequencies included (a), with all frequencies included (b), and for the NJL model (c). In each case, the diquark-condensed phase with $\Delta \neq 0$ is separated from that with $\Delta = 0$ by a second-order line. In Figs. 1 (a) and (b), Σ is the vacuum chiral field in the limit $m = 0$. In Fig. 1 (c), Λ is the momentum cutoff used in the NJL model. In each of the three cases, T_0 is the critical temperature for $\mu = 0$ and in the chiral limit $m = 0$.

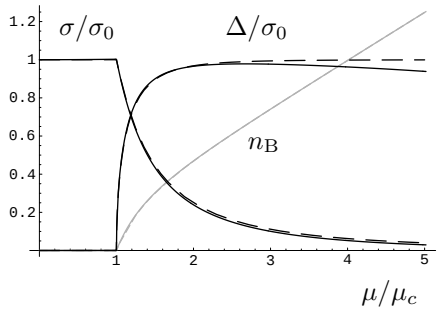

(a)

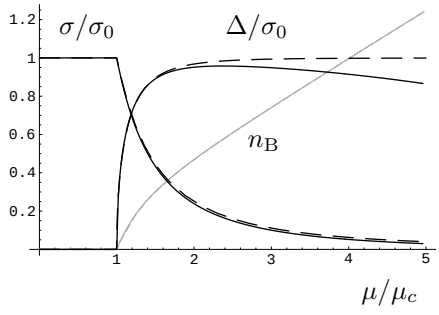

(b)

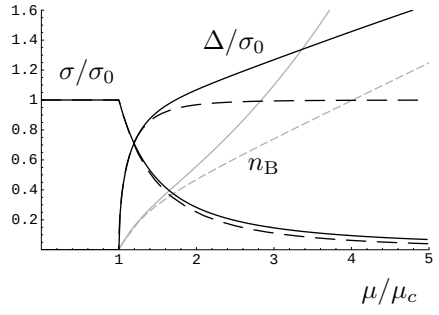

(c)

FIG. 2. Condensation fields near the edge $(\mu, T) = (\mu_c, 0)$ in the random matrix models with two Matsubara frequencies (a), all Matsubara frequencies (b), and in the NJL model (c). In each case, the dashed lines represent the predictions from chiral perturbation theory and the continuous lines are the results from the models considered in this paper. In each panel, σ_0 is the chiral field at $\mu = 0$. The grey curves represent the densities as a function of μ, scaled so that their slope is unity at the edge $\mu = \mu_c$. Note that the density curves from chiral perturbation theory overlap with those from the random matrix models ((a) and (b)).

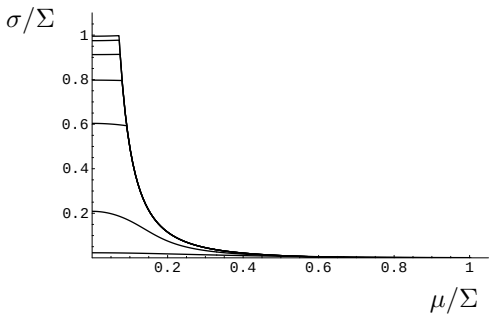

(a)

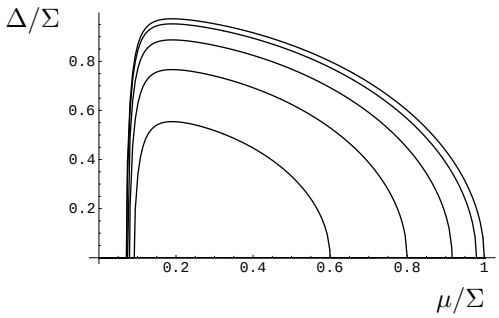

(b)

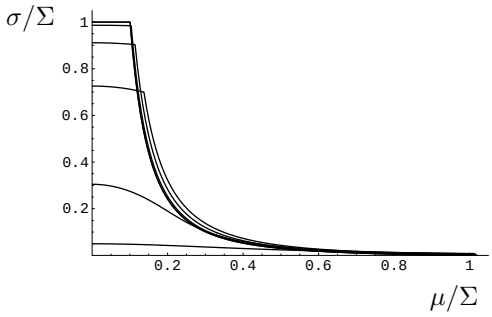

(c)

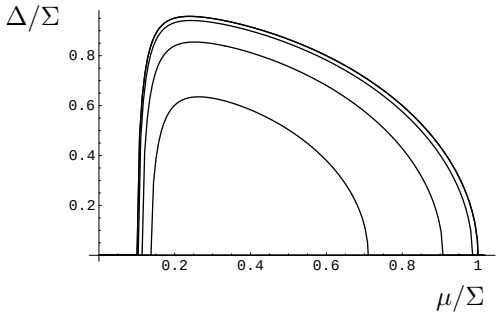

(d)

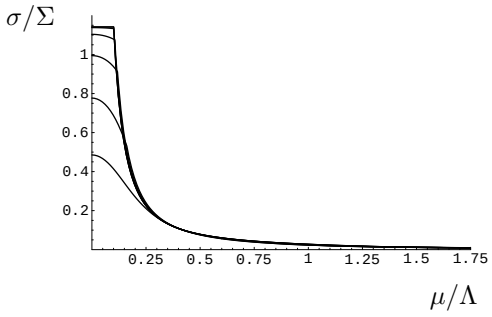

(e)

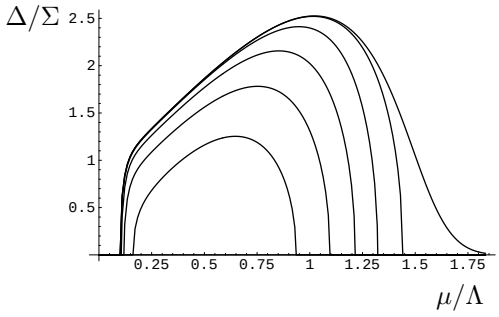

(f)

FIG. 3. Chiral and diquark fields for selected temperatures in the random matrix model with two Matsubara frequencies included ((*a*) and (*b*)), with all Matsubara frequencies included ((*c*) and (*d*)), and in the NJL model ((*e*) and (*f*)). In a given graph, the outer curve corresponds to $T = 0$. Going inward, the inner curves correspond to $T/T_0 = 0.2, 0.4, 0.6, 0.8, 1.0, 1.2$, where T_0 is the critical temperature for $\mu = 0$ and $m = 0$. Note that the σ curves slightly overlap in (*c*) for $T/T_0 = 0$ and $T/T_0 = 0.2$ and those in (*e*) slightly overlap for $T/T_0 = 0, 0.2$, and $T/T_0 = 0.4$. In Figs. 3 (*b*), (*d*), and (*f*), the diquark field vanishes for a few of the highest selected temperatures. In each graph, Σ is the vacuum chiral field in the limit $m = 0$; in Figs. 3 (*e*) and (*f*), Λ is the momentum cutoff used in the NJL model.